Photoelectron spectroscopy and density functional calculations of CuSin− (n = 4–18) clusters

Hong-Guang Xu, Miao Miao Wu, Zeng-Guang Zhang, Jinyun Yuan, Qiang Sun et al.

Citation: J. Chem. Phys. **136**, 104308 (2012); doi: 10.1063/1.3692685
View online: http://dx.doi.org/10.1063/1.3692685
View Table of Contents: http://jcp.aip.org/resource/1/JCPSA6/v136/i10
Published by the American Institute of Physics.

Photoelectron spectroscopy and density functional calculations of $CuSi_n^-$ (n = 4–18) clusters

Hong-Guang Xu,[1] Miao Miao Wu,[2] Zeng-Guang Zhang,[1] Jinyun Yuan,[1] Qiang Sun,[2,a)] and Weijun Zheng[1,a)]

[1]*Beijing National Laboratory for Molecular Sciences, State Key Laboratory of Molecular Reaction Dynamics, Institute of Chemistry, Chinese Academy of Sciences, Beijing 100190, China*

[2]*Department of Materials Science and Engineering and Center for Applied Physics and Technology, Peking University, Beijing 100871, China*

(Received 28 September 2011; accepted 20 February 2012; published online 14 March 2012)

We conducted a combined anion photoelectron spectroscopy and density functional theory study on the structural evolution of copper-doped silicon clusters, $CuSi_n^-$ (n = 4–18). Based on the comparison between the experiments and theoretical calculations, $CuSi_{12}^-$ is suggested to be the smallest fully endohedral cluster. The low-lying isomers of $CuSi_n^-$ with $n \geq 12$ are dominated by endohedral structures, those of $CuSi_n^-$ with $n < 12$ are dominated by exohedral structures. The most stable structure of $CuSi_{12}^-$ is a double-chair endohedral structure with the copper atom sandwiched between two chair-style Si_6 rings or, in another word, encapsulated in a distorted Si_{12} hexagonal prism cage. $CuSi_{14}^-$ has an interesting C_{3h} symmetry structure, in which the Si_{14} cage is composed by three four-membered rings and six five-membered rings. © *2012 American Institute of Physics*. [http://dx.doi.org/10.1063/1.3692685]

I. INTRODUCTION

Transition metal (TM)-doped silicon clusters have been studied extensively with experiments[1–15] and theoretical calculations[16–39] because they have novel properties and may serve as the building blocks for the fabrication of new nanostructures.[40–45] Cu-doped silicon clusters have received particular attention also due to the importance of silicon and copper in the semiconductor and microelectronic industries. Copper can diffuse into silicon wafer and react with the defects, therefore, reduce the lifetime of excited charge carriers in semiconductor devices.[46] In addition, it has been found that copper impurity can degrade the efficiency of silicon solar cells.[47] But it is very expensive to produce high purity solar-grade silicon. One way to improve the efficiency of silicon solar cells without using high-purity silicon might be manufacturing radial p-n junction solar cells from metallurgical-grade silicon (MGS) or upgraded-MGS which contains metal impurities such as Cu, Fe, Al, etc.[48] Exploring the structural and electronic properties of Cu-doped silicon can provide valuable information not only for developing cluster-assembled materials but also for improving microelectronic devices and solar cells.

The pioneering mass spectrometric study of Cu-doped silicon clusters was conducted by Beck[49] using the technique of laser vaporization supersonic expansion. In recent years, Cu-doped silicon clusters have been studied by a number of experiments. Duncan and co-workers[50] investigated the photodissociation of Cu-doped silicon clusters and found the dissociation of $CuSi_7^+$ and $CuSi_{10}^+$ clusters proceeded primarily by loss of a copper atom, indicating that the copper atom is not located inside the silicon cages. Lievens and co-workers[51] analyzed the mass spectrometric stabilities of a series of MSi_n^+ (M = Cr, Mn, Cu, Zn) clusters and found that the $CuSi_{6,7,10}^+$ clusters are relatively abundant. The same authors also investigated argon physisorption on TM-doped silicon clusters and showed that argon physisorption on $CuSi_n^+$ clusters dropped significantly at n = 12.[52] More recently, they measured the far-infrared vibrational spectra of MSi_n^+ (M = Cu, V) for cluster size up to n = 11 using argon-tagging infrared multiple photon dissociation (IR-MPD) technique.[53,54]

Many theoretical studies have also been conducted to explore the structures and properties of Cu-doped silicon clusters. The geometry, stability, and bonding properties of small $CuSi_n$ (n = 1–6) clusters have been investigated by Xiao *et al.*,[55,56] Ovcharenko *et al.*,[57] Liu *et al.*,[58] and Dkhissi.[59] The middle size $CuSi_n$ clusters in the range of n = 8–16 have been extensively studied by many theoretical groups.[60–73] Although most of the theoretical calculations are in good agreement with each other, there are some controversies regarding the structure of $CuSi_{10}$ cluster and the critical size for the emergence of endohedral structures. For example, Xiao *et al.*[62] investigated the geometric, energetic, and bonding properties of $CuSi_n^{+/0/-}$ (n = 4, 6, 8, 10, 12) clusters using density functional method and found five nearly isoenergetic exohedral structures for $CuSi_{10}$ cluster. However, more recent theoretical calculations[68] showed an approximately D_{5h} endohedral structure for $CuSi_{10}$. It has been proposed that Si_9 might be the smallest Si cage that can encapsulate a copper atom. But that has not been proved by the existing experiments. On the other hand, it is interesting to note that theoretical calculations[62,63,66–68,72] predicted a so-called double-chair endohedral structure for $CuSi_{12}$ cluster, which is worth further experimental

a)Authors to whom correspondence should be addressed. Electronic addresses: sunqiang@pku.edu.cn and zhengwj@iccas.ac.cn.

confirmation. In order to provide more detailed information about the evolution of the structural and electronic properties of copper-doped silicon clusters, we investigated the $CuSi_n^-$ (n = 4–18) clusters using anion photoelectron spectroscopy combined with density functional calculations in this work.

II. EXPERIMENTAL AND THEORETICAL METHODS

A. Experimental

The experiments were conducted on a home-built apparatus equipped with a laser vaporization supersonic cluster source, a linear time-of-flight mass spectrometer, and a magnetic-bottle photoelectron spectrometer, which has been described in Ref. 13. The $CuSi_n^-$ cluster anions were generated in the laser vaporization source by laser ablation of a rotating translating disk target (13 mm diameter, Cu/Si mole ratio 1:4) with the second harmonic of a nanosecond Nd:YAG laser (Continuum Surelite II-10). The typical laser power used in this work is about 10 mJ/pulse. Helium gas with ~4 atm. backing pressure was allowed to expand through a pulsed valve (General Valve Series 9) into the source to cool the formed clusters. The generated cluster anions were mass-analyzed with the linear time-of-flight mass spectrometer. The cluster anions of interest were selected with a mass gate, decelerated by a momentum decelerator, and crossed with the beam of an Nd:YAG laser (Continuum Surelite II-10, 266 nm) or an excimer laser (ArF: 193 nm) at the photodetachment region. The electrons from photodetachment were energy-analyzed by the magnetic-bottle photoelectron spectrometer. The resolution of the magnetic-bottle photoelectron spectrometer was about 40 meV at electron kinetic energy of ~1 eV. The photoelectron spectra were calibrated with known spectra of Cu^- and Au^-. In this work, the mass and photoelectron signals were amplified by a broadband amplifier, digitized with a digital card, and monitored with a laboratory computer. The background noise of the photoelectron spectra was subtracted shot by shot.

B. Theoretical

The calculations were carried out within the framework of density-functional theory (DFT), where the Becke's three-parameter and Lee–Yang–Parr's gradient-corrected correlation hybrid functional (B3LYP) and 6-311+G(d) basis sets were used for structural optimization and frequency calculations[74,75] as implemented in GAUSSIAN 03 (G03).[76] For comparison, generalized gradient approximation with the Perdew-Wang 91 (PW91) form[77] was also tested. It was found that the results from the B3LYP method are in slightly better agreement with the experiment. Here, we present the results from the B3LYP functional. The initial structures of $CuSi_n^-$ clusters for geometry optimizations were obtained from the $CuSi_n^{-,0,+}$ clusters reported in the literature and were also obtained by putting the Cu atom to different adsorption or substitution sites of the low-lying isomers of pure silicon clusters reported in the literature. All geometry optimizations were conducted without any symmetry constraint. Spin singlet states of $CuSi_n^-$ (n = 4–18) cluster anions and doublet states of their corresponding neutrals were considered. Harmonic vibrational frequencies were calculated to make sure that the structures correspond to the real local minima. The zero-point vibrational energy corrections were included for the relative energies of the isomers.

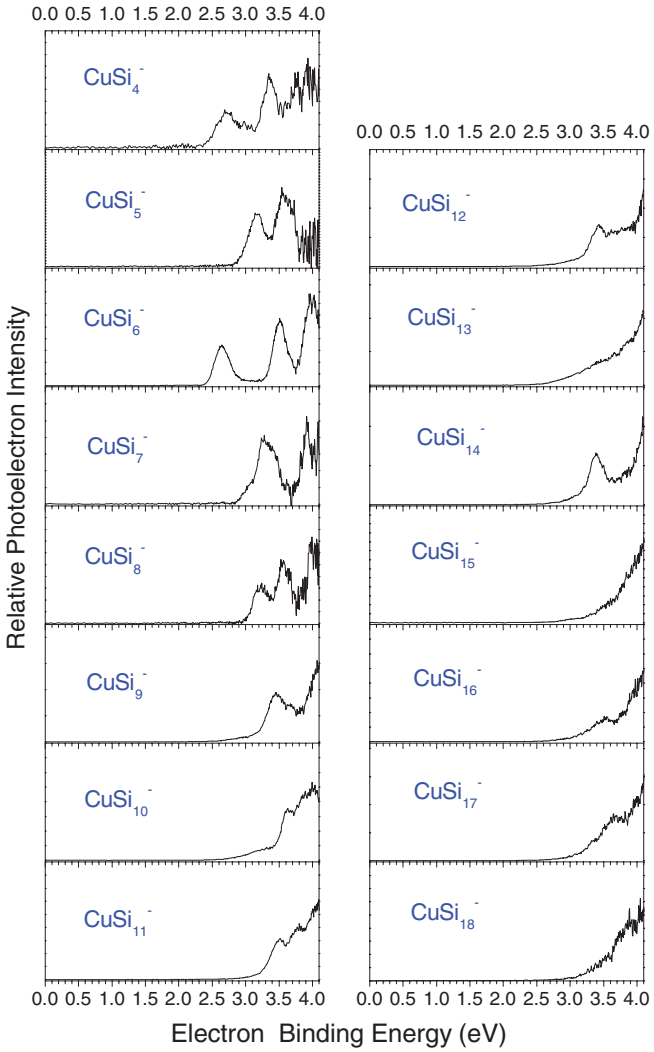

FIG. 1. Photoelectron spectra of $CuSi_n^-$ (n = 4–18) clusters recorded with 266 nm photons.

III. EXPERIMENTAL RESULTS

The photoelectron spectra of $CuSi_n^-$ (n = 4–18) clusters recorded with 266 nm (4.661 eV) photons are presented in Figure 1, and those recorded with 193 nm (6.424 eV) photons are shown in Figure 2. The spectra taken with 193 nm photons show the spectral features at higher binding energy. The spectral peaks in the 193 nm spectra are broader than those in the 266 nm spectra since the kinetic energies of the photoelectrons produced by the 193 nm photons are higher than those by the 266 nm photons. The vertical detachment energies (VDEs) and the adiabatic detachment energies (ADEs) of the cluster anions estimated from the photoelectron spectra are listed in Table I. The ADE from each spectrum was determined by drawing a straight line along the leading edge of the

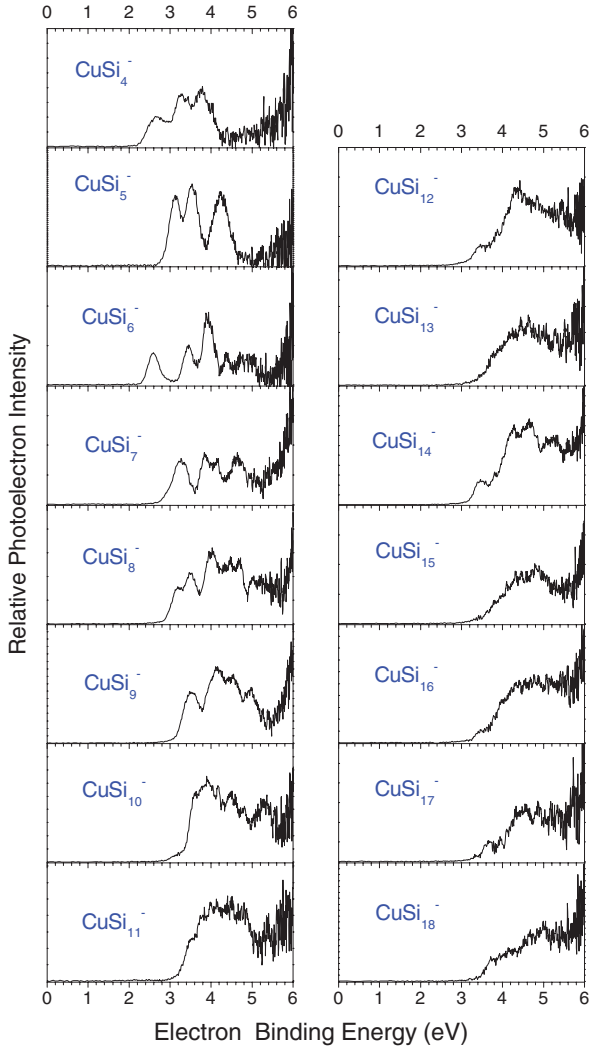

FIG. 2. Photoelectron spectra of $CuSi_n^-$ (n = 4–18) clusters recorded with 193 nm photons.

first peak to cross the baseline of the spectrum and adding the instrumental resolution to the electron binding energy (EBE) value at the crossing point. The VDEs were estimated from the maxima of the first peaks. The spectra of small $CuSi_n^-$ (n = 4–9) clusters in general are better resolved than those of larger $CuSi_n^-$ (n = 10–18) clusters. We can distinguish many spectral peaks in the spectra from $CuSi_4^-$ to $CuSi_9^-$. $CuSi_4^-$ has three major peaks centered at 2.69, 3.35, and 3.78 eV. $CuSi_5^-$ has three major peaks centered at 3.15, 3.58, and 4.25 eV. $CuSi_6^-$ has six major features centered at 2.64, 3.51, 3.95, 4.38, 4.70, and 5.00 eV. $CuSi_7^-$ has four major peaks centered at 3.25, 3.90, 4.14, and 4.65 eV. $CuSi_8^-$ has seven features at 3.22, 3.58, 4.02, 4.47, 4.69, 5.01, and 5.22 eV. $CuSi_9^-$ has peaks at approximately 3.44, 4.12, 4.52, and 4.96 eV. It is relatively difficult to determine the spectra features of $CuSi_{10\text{-}18}^-$ clusters because the spectral features become broad starting from n = 10. But it is worth pointing out that, for the spectra of $CuSi_{12}^-$ and $CuSi_{14}^-$, an obvious low binding feature can be observed at 3.42 and 3.38 eV, respectively. That may indicate that the structures of $CuSi_{12}^-$ and $CuSi_{14}^-$ have relatively higher symmetry.

TABLE I. Vertical detachment energies (VDEs) and adiabatic detachment energies (ADEs) of the $CuSi_n^-$ (n = 4–18) clusters estimated from their photoelectron spectra.

n	VDE (eV)	ADE (eV)
4	2.69 ± 0.08	2.40 ± 0.08
5	3.15 ± 0.08	2.90 ± 0.08
6	2.64 ± 0.08	2.43 ± 0.08
7	3.25 ± 0.08	2.90 ± 0.08
8	3.22 ± 0.08	3.04 ± 0.08
9	3.44 ± 0.08	3.22 ± 0.08
10	3.62 ± 0.08	3.46 ± 0.08
11	3.50 ± 0.08	3.23 ± 0.08
12	3.42 ± 0.08	3.24 ± 0.08
13	3.7 ± 0.2	3.4 ± 0.2
14	3.38 ± 0.08	3.22 ± 0.08
15	3.8 ± 0.2	3.4 ± 0.2
16	3.51 ± 0.08	3.16 ± 0.08
17	3.63 ± 0.08	3.15 ± 0.08
18	3.7 ± 0.2	3.4 ± 0.2

The VDEs and ADEs of $CuSi_{13}^-$, $CuSi_{15}^-$, and $CuSi_{18}^-$ are estimated from their 193 nm photoelectron spectra. Those of the other $CuSi_n^-$ clusters are estimated from their 266 nm photoelectron spectra.

IV. THEORETICAL RESULTS AND DISCUSSION

In order to get insight into the structures of Cu-doped silicon clusters, we optimized geometries of the low-lying isomers for $CuSi_n^-$ (n = 4–18) with DFT calculations and presented them in Figures 3 and 4 with the most stable structures on the left. The relative energies between these isomers as well as their theoretical VDEs and ADEs are summarized in Table II. The cartesian coordinates of the stable isomers can be found in the supplementary material.[78] It can be seen from Figures 3 and 4 that the structures of $CuSi_n^-$ clusters with n < 12 are dominated by exohedral structures and those with n ≥ 12 are dominated by endohedral structures.

We have also simulated the photoelectron spectra of different isomers based on theoretically generalized Koopman theorem,[79,80] in which each transition corresponds to removal of an electron from a specific molecular orbital of the cluster anions. In the simulation, we first set the transition related to the highest occupied molecular orbital (HOMO) of the cluster anion to the position of VDE, and shifted the transitions of the deeper orbitals according to the HOMO transition. For convenient, we call the simulated spectra as density of states (DOS) spectra.[80] The DOS spectra and experimental spectra are compared in Figure 5. The simulated DOS spectra fit the experimental spectra quite well because the $CuSi_n^-$ clusters have close-shell electronic structures and the theoretical treatment is more reliable for the close-shell electronic structures.

A. $CuSi_4^-$

As shown in Figure 3, $CuSi_4^-$ has three stable isomers (4A, 4B, and 4C) with C_s symmetry. The most stable isomer (4A) can be described as the Cu atom attaching to the vertex of Si_4 rhombus. The second stable isomer (4B) has a compressed trigonal bipyramidal structure. Isomer 4B is less stable than isomer 4A by 0.15 eV. The calculated VDEs

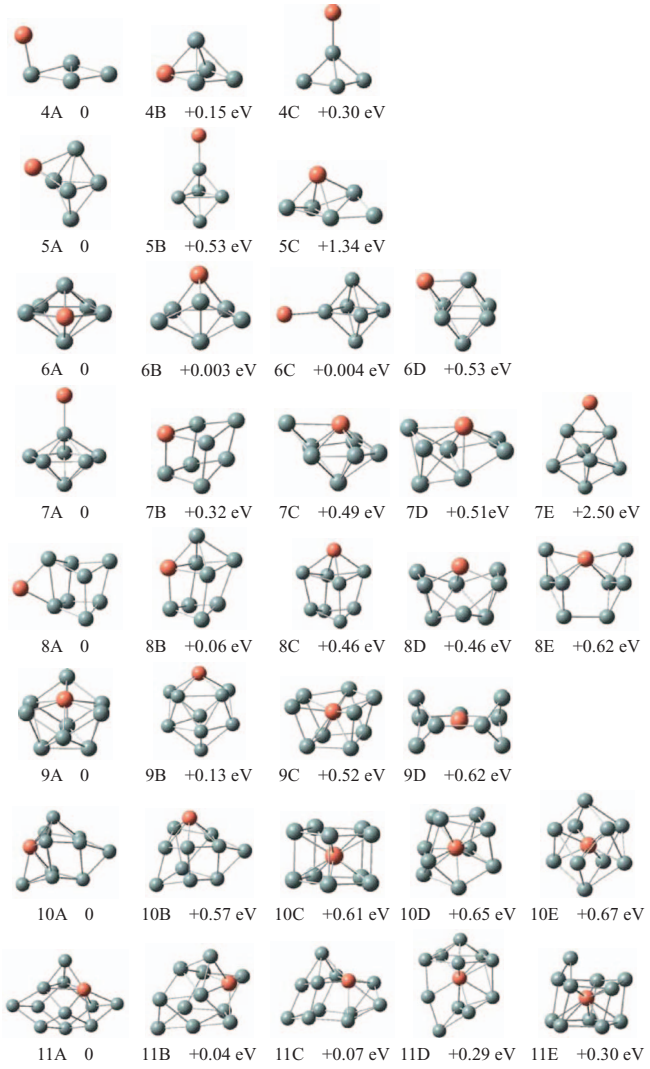

FIG. 3. Optimized geometries of the typical low-lying isomers of $CuSi_n^-$ (n = 4–11) clusters. The relative energies to the most stable isomers are shown. The dark cyan and red brown spheres stand for Si and Cu atoms, respectively.

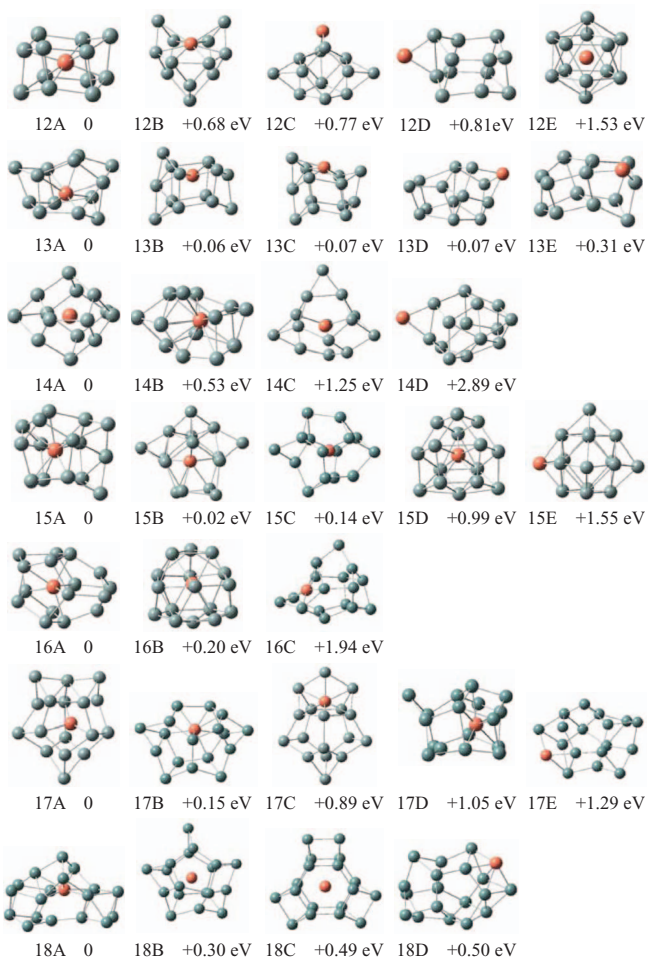

FIG. 4. Optimized geometries of the typical low-lying isomers of $CuSi_n^-$ (n = 12–18) clusters. The relative energies to the most stable isomers are shown. The dark cyan and red brown spheres stand for Si and Cu atoms, respectively.

of isomers 4A and 4B are 2.58 and 2.52 eV, respectively, in agreement with the experimental value (2.69 eV). Isomer 4C has the Cu atom connect to the apex of the Si_4 tetrahedron. It is less stable than isomer 4A by 0.3 eV. Its VDE is calculated to be 2.81 eV, higher than the experimental value by 0.12 eV. From Figure 5, we can see that the simulated DOS spectrum of isomer 4B resembles the experimental spectrum of $CuSi_4^-$ very well. Therefore, we would like to suggest isomer 4B to be the major isomer detected in the experiment although it is slightly higher than isomer 4A in energy. Isomer 4A probably contributed very little to the experimental spectrum. The structure of isomer 4A is similar to that calculated by Xiao *et al.*[56,62] The theoretical VDE (2.591 eV) calculated by Xiao *et al.*[62] is also close to our experimental value. Ona *et al.*[64] also found a stable isomer similar to isomer 4A for $CuSi_4$ neutral.

B. $CuSi_5^-$

The most stable isomer of $CuSi_5^-$, 5A, can be considered as adding a face-capping copper atom to Si_5 trigonal bipyramid. Isomer 5B has the Cu atom connecting to the vertex of the Si_5 trigonal bipyramid. Isomer 5C has a Si atom connecting to one of the edges of the trigonal bipyramid formed by $CuSi_4$. The VDE and ADE of isomer 5A are calculated to be ~3.01 and ~2.69 eV, respectively, consistent with the experimental measurements (3.15 and 2.90 eV). The theoretical VDE of isomer 5B is close to the experimental value, but it is less stable than isomer 5A by 0.53 eV. Isomer 5C is less stable than isomer 5A by 1.34 eV. Also, its theoretical VDE is much smaller than the experimental value. Consequently, the existence of isomers 5B and 5C in our experiments can be ruled out. We suggest isomer 5A to be the most probable structure for $CuSi_5^-$. The simulated DOS spectrum of isomer 5A is in good agreement with the experiment. The structure of isomer 5A is in agreement with the theoretical calculations conducted by Xiao *et al.*[56] and Chuang *et al.*[73]

C. $CuSi_6^-$

Our calculations show that the first three isomers of $CuSi_6^-$, 6A, 6B, and 6C, are degenerate in energy. Isomer 6A

TABLE II. Relative energies of the low-lying isomers of $CuSi_n^-$ (n = 4–18) as well as their VDEs and ADEs obtained by DFT calculations (B3LYP/6-311+G(d)). The isomers labeled in bold are the most probable isomers in the experiment.

Isomer		Symmetry	ΔE (eV)	VDE (eV)		ADE (eV)		Isomer		Symmetry	ΔE (eV)	VDE (eV)		ADE (eV)	
				Theory	Expt.	Theory	Expt.					Theory	Expt.	Theory	Expt.
$CuSi_4^-$	4A	C_s	0	2.58	2.69	2.37	2.40	$CuSi_{12}^-$	**12A**	C_{3v}	0	3.34	3.42	3.17	3.24
	4B	C_s	0.15	2.52		2.48			12B	C_1	0.68	3.18		3.05	
	4C	C_s	0.30	2.81		2.39			12C	C_s	0.77	3.34		3.11	
$CuSi_5^-$	**5A**	C_s	0	3.01	3.15	2.69	2.90		12D	C_s	0.81	3.51		3.32	
	5B	C_{3v}	0.53	3.02		2.80			12E	D_{3d}	1.53	3.54		3.26	
	5C	C_1	1.34	2.51		1.33		$CuSi_{13}^-$	**13A**	C_1	0	3.55	3.7	3.55	3.4
$CuSi_6^-$	**6A**	C_{2v}	0	2.52	2.64	2.39	2.43		**13B**	C_s	0.06	3.54		3.32	
	6B	C_s	0.003	2.61		2.31			**13C**	C_s	0.07	3.38		3.32	
	6C	C_{4v}	0.004	3.05		2.58			**13D**	C_s	0.07	3.53		3.30	
	6D	C_{3v}	0.53	2.65		2.37			13E	C_1	0.31	3.51		3.17	
$CuSi_7^-$	**7A**	C_{5v}	0	3.05	3.25	2.74	2.90	$CuSi_{14}^-$	**14A**	C_{3h}	0	3.41	3.38	3.19	3.22
	7B	C_s	0.32	2.85		2.41			14B	C_1	0.53	3.37		3.16	
	7C	C_s	0.49	2.58		2.32			14C	C_1	1.25	3.12		2.99	
	7D	C_1	0.51	2.88		2.72			14D	C_1	2.89	3.14		2.45	
	7E	C_{2v}	2.50	2.44		1.97		$CuSi_{15}^-$	**15A**	C_1	0	3.21	3.8	3.08	3.4
$CuSi_8^-$	**8A**	C_s	0	3.35	3.22	3.03	3.04		**15B**	C_1	0.02	3.38		3.01	
	8B	C_s	0.06	3.17		2.95			**15C**	C_1	0.14	3.35		3.17	
	8C	C_2	0.46	3.08		2.91			15D	C_s	0.99	3.37		3.12	
	8D	C_s	0.46	3.27		2.90			15E	C_s	1.55	3.61		3.42	
	8E	C_{2v}	0.62	3.38		2.86		$CuSi_{16}^-$	**16A**	C_1	0	3.35	3.51	3.15	3.16
$CuSi_9^-$	**9A**	C_{3v}	0	3.57	3.44	3.28	3.22		16B	C_1	0.20	3.61		3.13	
	9B	C_s	0.13	3.48		3.14			16C	C_1	1.94	3.50		3.12	
	9C	C_1	0.52	3.18		2.95		$CuSi_{17}^-$	**17A**	C_1	0	3.17	3.63	3.01	3.15
	9D	C_s	0.62	3.44		3.16			**17B**	C_1	0.15	3.48		3.31	
$CuSi_{10}^-$	**10A**	C_s	0	3.47	3.62	3.32	3.46		17C	C_s	0.89	3.48		3.13	
	10B	C_s	0.57	2.79		2.68			17D	C_1	1.05	3.26		2.79	
	10C	D_{5h}	0.61	2.91		2.83			17E	C_1	1.29	3.38		2.44	
	10D	C_s	0.65	3.30		2.75		$CuSi_{18}^-$	**18A**	C_s	0	3.64	3.7	3.36	3.4
	10E	C_1	0.67	2.95		2.72			18B	C_1	0.30	3.42		2.83	
$CuSi_{11}^-$	**11A**	C_1	0	3.36	3.50	3.13	3.23		18C	D_3	0.49	3.47		3.28	
	11B	C_1	0.04	3.08		2.78			18D	C_1	0.50	3.21		2.79	
	11C	C_1	0.07	3.27		2.98									
	11D	C_s	0.29	3.48		2.84									
	11E	C_s	0.30	3.20		2.84									

has a pentagonal bipyramidal structure with C_{2v} symmetry, and isomer 6B is a distorted pentagonal bipyramidal structure with C_s symmetry. Isomer 6C has the Cu atom connecting to the vertex of the Si_6 octahedron. The calculated VDEs of isomers 6A (2.52 eV) and 6B (2.61 eV) are in accordance with the experimental value. The VDE of isomer 6C is calculated to be 3.05 eV, which is much higher than the experimental value (2.64 eV). Isomer 6D can be considered as a Si_6 octahedron face-capped by a Cu atom. Its VDE is close to the experimental measurement but it is less stable than isomer 6A by 0.53 eV. It is unlikely for isomer 6D to be present in the experiments. We suggest that isomers 6A and 6B coexist in our experiments since they are very close in energy and their simulated DOS spectra are in good agreement with experimental spectrum of $CuSi_6^-$. Xiao *et al.*[56,62] found two stable isomers similar to isomers 6A and 6B in this work. Their calculated VDEs for these two isomers (2.513 and 2.606 eV) (Ref. 62) are also consistent with our experimental value. The structure of isomer 6A is also similar to the structure of $CuSi_6^+$ reported by Lievens and co-workers.[54]

D. $CuSi_7^-$

The most stable isomer of $CuSi_7^-$ (7A) has C_{5v} symmetry with the Cu atom connecting to the top of the Si_7 pentagonal bipyramid. The calculated VDE and ADE of isomer 7A are 3.05 and 2.74 eV, respectively, in reasonable agreement with the experimental measurements (3.25 and 2.90 eV). Isomers 7B, 7C, 7D, and 7E are less stable than isomer 7A by 0.32, 0.49, 0.51, and 2.50 eV, respectively. Their calculated VDEs are 2.85, 2.58, 2.88, and 2.44 eV, respectively, much lower than the experimental value. Isomer 7A is the most probable isomer detected in the experiments. From Figure 5, we can see that some of the photoelectron features in the experimental spectrum of $CuSi_7^-$ cannot be matched by simulated DOS spectrum of isomer 7A alone. It might be possible that isomer 7B also exist in the experiment. Chuang *et al.*[73] suggested that the most stable isomer of $CuSi_7$ neutral has the Cu atom binding to the edge of the Si_7 pentagonal bipyramid and co-planar with the Si_5 pentagon, which is the same as isomer 7E. Isomer 7E is also similar to the structure of $CuSi_7^+$ cation found by Lievens and

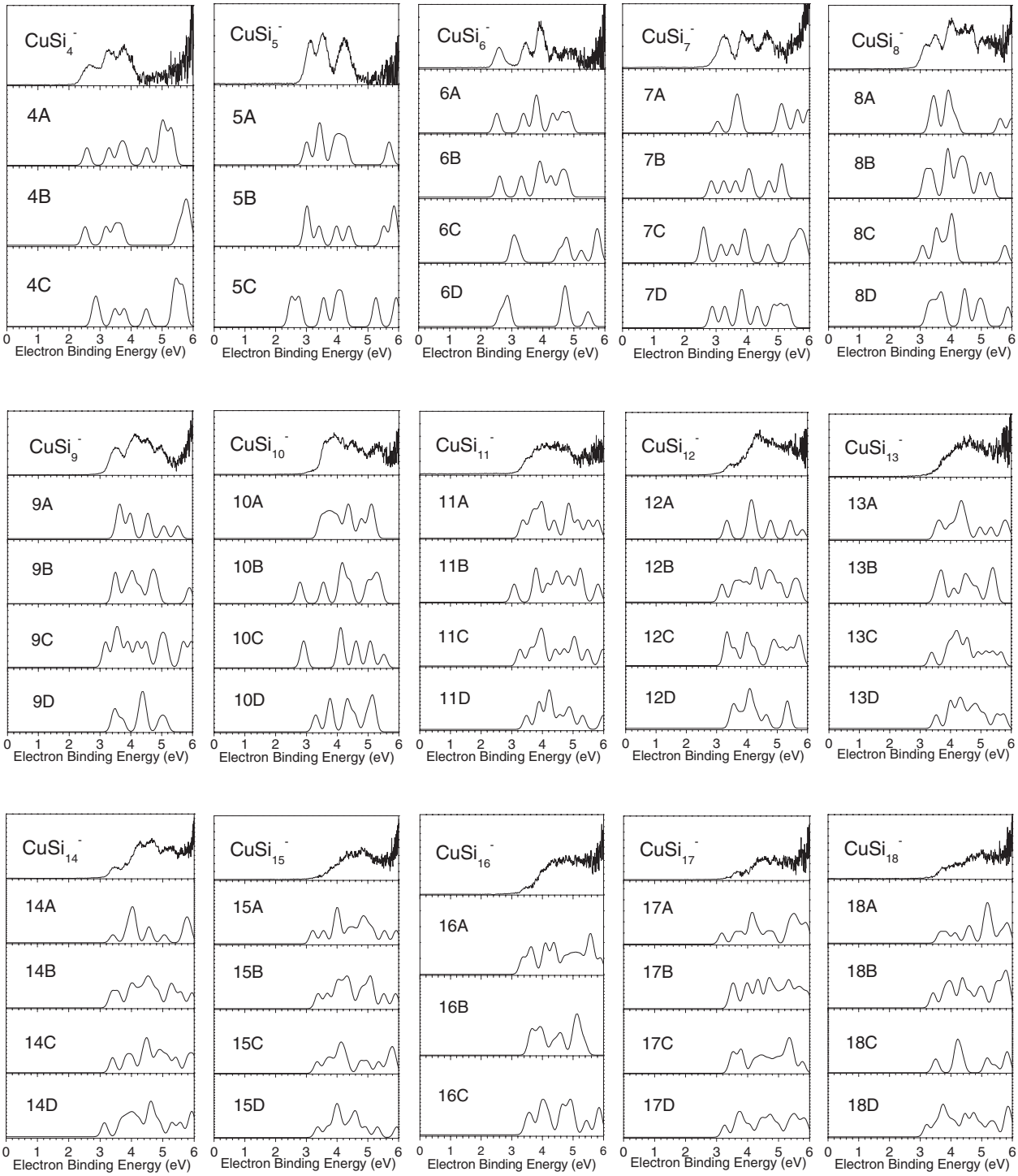

FIG. 5. Comparison between the experimental photoelectron spectra and the simulated DOS spectra of the low-lying isomers of $CuSi_n^-$ ($4 \le n \le 18$) clusters. The simulations were conducted by fitting the distribution of the transition lines with unit-area Gaussian functions of 0.25 eV width.

co-workers.[54] However, our calculations show that isomer 7E of $CuSi_7^-$ anion is less stable. The 7E structure of $CuSi_7^+$ cation probably is stabilized by the strong interaction between the positive charged Cu with the Si atoms.

E. $CuSi_8^-$

Five stable isomers of $CuSi_8^-$ are shown in Figure 3. The most stable one, isomer 8A, has C_s symmetry with the Cu atom attaching to the edge of the distorted Si_8 tetragonal prism. Isomer 8B is higher than isomer 8A by 0.06 eV in energy. It can be viewed as a silicon atom attaching to the top of a distorted Si_8 tetragonal prism then having one of the silicon atoms in the distorted Si_8 tetragonal prism replaced by a Cu atom. Isomer 8C is higher than isomer 8A by 0.46 eV in energy. It has the Cu atom attaching to the top of the distorted Si_8 tetragonal prism. Isomers 8D and 8E are higher than isomer 8A by 0.46 and 0.62 eV in energy, respectively. They can be

considered as a Cu atom interacting with a boat-shaped structure formed by the eight Si atoms. The theoretical VDEs of isomers 8A–8E are calculated to be 3.35, 3.17, 3.08, 3.27, and 3.38 eV, respectively. They are all in reasonable agreement with the experimental value (3.22 eV). However, isomers 8C, 8D, and 8E are much less stable than isomers 8A and 8B. Thus, we suggest that isomers 8A and 8B are the most probable isomers in our experiments. Based on the simulated DOS spectra in Figure 5, the combination of isomers 8A and 8B can produce the experimental spectrum of $CuSi_8^-$. Isomers 8A and 8B have been identified as the competitive candidates for the most stable structures of $CuSi_8^-$ by Xiao *et al.*[62] Besides, the theoretical VDEs calculated by Xiao *et al.*[62] also agree nicely with our experimental measurement. Chuang *et al.*[73] calculations suggest isomer 8B to be the most stable structure for $CuSi_8$ neutral. Although the structures of isomers 8A and 8B are different from the structure of $CuSi_8^+$ found by Lievens and co-workers,[54] our results are in agreement with their findings that the Cu atom occupies an exterior site.

F. $CuSi_9^-$

The first two isomers of $CuSi_9^-$, 9A and 9B are very close in energy. Isomer 9B is higher than isomer 9A by only 0.13 eV. They are both exohedral structures with the Cu atom occupying an exterior site of the silicon framework. The theoretical calculations also show two endohedral isomers for $CuSi_9^-$. They are isomers 9C and 9D. But they are less stable than isomer 9A by 0.52 and 0.62 eV, respectively. The calculated VDEs of isomers 9A, 9B, 9C, and 9D are 3.57, 3.48, 3.18, and 3.44 eV, respectively. They are all very close to experimental VDE (3.44 eV) except that of isomer 9C is lower than the experimental value by 0.26 eV. Since isomers 9C and 9D are much less stable, we suggest that isomers 9A and 9B are the most probable isomers detected in the experiments. Based on the simulated DOS spectra in Figure 5, the combination of isomers 9A and 9B can produce the experimental spectrum of $CuSi_9^-$. The theoretical calculations by Hossain *et al.*[68] and Lan *et al.*[71] found a stable isomer with the Cu atom encapsulated by the Si_9 cage, which is similar to isomer 9C. However, our calculations show that this endohedral structure is much less stable than isomer 9A. It is unlikely for it to be present in our experiments. Isomers 9A and 9B are similar to iso3–5 of $CuSi_9^+$ reported by Lievens and co-workers.[54]

G. $CuSi_{10}^-$

For $CuSi_{10}^-$, isomers 10A and 10B can be viewed as the Cu atom substitutes a silicon atom of the Si_{11} framework. Isomer 10B is less stable than isomer 10A by 0.57 eV. The Cu atom is not encapsulated by silicon cage in either isomers 10A or 10B. The theoretical VDE of isomer 10A is calculated to be 3.47 eV, which is in good agreement with the experimental value (3.62 eV). That of isomer 10B is calculated to be 2.79 eV, much lower than the experimental value. Isomers 10C, 10D, and 10E are endohedral structures with D_{5h}, C_s, and C_1 symmetry, respectively. These endohedral structures are much less stable than isomer 10A. Our calculations show that they are higher than isomer 10A by at least 0.61 eV in energy. Their theoretical VDEs also deviate from the experiment value. Therefore, the existence of endohedral structures for $CuSi_{10}^-$ may not be possible in the experiments. Isomer 10A is the most probable isomer detected in our experiments. The simulated DOS spectrum of isomer 10A is in good agreement with experiment spectrum of $CuSi_{10}^-$. There were some disagreements in the literature regarding the structure of $CuSi_{10}$ cluster. King[81] proposed a 10-vertex D_{4d} polyhedron endohedral structure for $CuSi_{10}$, which is similar to isomer 10E in this work. The DFT calculations conducted by Zdetsis[66] found the D_{4d} endohedral structure has imaginary frequencies and can be relaxed to two lower isoenergetic endohedral isomers of C_{2v} and C_s symmetry. Xiao *et al.*[62] found that the endohedral isomers of $CuSi_{10}$ anion and neutral are slightly less stable than their exohedral isomers. Very recently, Hossain *et al.*[68] proposed a D_{5h} endohedral structure to be the lowest in energy. However, our calculations show that the D_{5h} endohedral structure, isomer 10C, is less stable than the exohedral structure (isomer 10A). Our results are in agreement with those of Xiao *et al.*[62] It is also worth mentioning that the recent photodissociation experiment of $CuSi_{10}^+$ also indicates that the Cu atom tends to occupy an exterior site.[50] Isomer 10A is similar to the structures of iso2 and iso3 of $CuSi_{10}^+$ reported by Lievens and co-workers.[54]

H. $CuSi_{11}^-$

The first three isomers of $CuSi_{11}^-$ are very close in energy. The Cu atom is not encapsulated in these isomers. Isomers 11B and 11C are higher than isomer 11A by only 0.04 and 0.07 eV, respectively. The VDEs of isomers 11A and 11C are very close to the experiment measurement. The VDE of isomer 11D deviates from the experimental value. Isomers 11D and 11E are endohedral structures with the Cu atom encapsulated by the silicon atoms. They are less stable than isomer 11A by about 0.29 and 0.30 eV, respectively. Their VDEs are calculated to be 3.48 and 3.20 eV close to the experimental value (3.50 eV). We suggest that isomers 11A and 11C probably present in our experiments. However, the existence of isomers 11D and 11E cannot be ruled out. From the simulated DOS spectra in Figure 5, it is possible that isomers 11A, 11B, 11C, and 11D all contribute to the experimental spectrum. The theoretical calculations conducted by Hossain *et al.*[68] and Lan *et al.*[71] found an endohedral structure with C_s symmetry, which is similar to isomer 11E. The most stable structure of $CuSi_{11}$ neutral calculated by Chuang *et al.*[73] is an exohedral structure similar to isomer 11B. Isomers 11A and 11B are similar to iso2 and iso1 of $CuSi_{11}^+$ reported by Lievens and co-workers.[54]

I. $CuSi_{12}^-$

Starting from $CuSi_{12}^-$, the endohedral structures of $CuSi_n^-$ clusters are more stable than their exohedral structures. As shown in Figure 4, the most stable isomer of $CuSi_{12}^-$ (12A) is an endohedral structure with the Cu atom sitting at the center of a cagelike hexagonal double-chair

formed by 12 Si atoms. The VDE of isomer 12A is calculated to be 3.34 eV, in good agreement with the experimental value (3.42 eV). The exohedral structures such as isomers 12B, 12C, and 12D are much less stable than isomer 12A. It is worth mentioning that $CuSi_{12}^-$ can also form a highly symmetric icosahedron structure (isomer 12E) with the Cu atom encapsulated at the center. But this structure is much less stable, it is higher than isomer 12A by ~1.53 eV. The theoretical VDEs of isomers 12B–12E are also in reasonable agreement with the experimental value. But it is unlikely for them to be present in our experiments since they are much less stable than isomer 12A. Thus, isomer 12A is the most probable one detected in our experiments. The simulated DOS spectrum of isomer 12A is in reasonable agreement with the experimental spectrum although the experimental spectrum of $CuSi_{12}^-$ is not at good resolution. The structure of $CuSi_{12}$ anion and neutral has been investigated intensively by theoretical calculations. Xiao *et al.*[61,62] and Hagelberg *et al.*[63] first proposed the cagelike hexagonal double-chair structure as the best candidate for the ground state of $CuSi_{12}$, which is as same as isomer 12A in this work. The theoretical VDE of $CuSi_{12}$ anion was calculated by Xiao *et al.*[62] to be 3.352 eV, which is also in accordance with our experimental value. The theoretical calculations conducted by some other groups also show a cagelike hexagonal double-chair structure for $CuSi_{12}$ as well[66–69,71,72] except for Ona *et al.*[64] and Chuang *et al.*[73]

J. $CuSi_{13}^-$

The first four isomers of $CuSi_{13}^-$ are very close in energy with isomers 13B, 13C, and 13D to be less stable than isomer 13A by only 0.06, 0.07, and 0.07 eV. Isomer 13E is higher than isomer 13A by ~0.31 eV. Isomers 13A and 13B are endohedral structures. Isomers 13C, 13D, and 13E has the Cu atom localizes on the surface of the silicon framework. The calculated VDEs of the isomers 13A and 13B are 3.55 and 3.54 eV, respectively, consistent with the experimental measurement (3.7 eV). The VDE of isomer 13C deviates from the experimental value. The VDEs of isomers 13D and 13E are close to the experimental value. We suggest that these isomers may coexist in the experiments. From the simulated DOS spectra in Figure 5, it is possible that isomers 13A, 13B, 13C, and 13D all contribute to the experimental spectrum. Hossain *et al.*[68] and Lan *et al.*[71] found a C_s symmetry endohedral structure similar to isomer 13B as the most stable isomer. Chuang *et al.*[73] showed an endohedral structure similar to isomer 13A. Since these two isomers are close in energy and the difference between their geometries is very small, the theoretical calculations can be considered as in good agreement.

K. $CuSi_{14}^-$

The first three isomers of $CuSi_{14}^-$ (14A, 14B, and 14C) are all endohedral structures with the Cu atom encapsulated inside the silicon cages. Particularly, isomer 14A has an interesting C_{3h} symmetric structure, in which the Si_{14} cage is composed by three four-membered rings and six five-membered rings. The four-membered rings and five-membered rings are bending and distorted slightly so that the Si atoms in the rings are not co-planar. The VDE of isomer 14A is calculated to be 3.41 eV, in good agreement with the experimental value (3.38 eV). The VDEs of isomers 14B and 14C are also close to the experimental value. But they are much less stable than isomer 14A. Their energies are higher than isomer 14A by 0.53 and 1.25 eV, respectively. Isomer 14D is an exohedral structure. It is much less stable and higher than isomer 14A by ~2.89 eV. The simulated DOS spectrum of isomer 14A is in agreement with the experimental spectrum of $CuSi_{14}^-$. We suggest isomer 14A to be the most probable isomer detected in the experiments. The structure of isomer 14A is identical to the most stable structure calculated by Hossain *et al.*,[68] Lan *et al.*,[71] and Chuang *et al.*[73]

L. $CuSi_{15}^-$

The first three isomers of $CuSi_{15}^-$ (15A, 15B, and 15C) are very close in energy. They are all endohedral structures. Isomers 15B and 15C are higher than isomer 15A by only 0.02 and 0.14 eV in energy. Isomer 15D is also an endohedral structure. It is higher than isomer 15A by 0.99 eV in energy. Isomer 15E is an exohedral structure and is less stable than isomer 15A by 1.55 eV. The VDEs of isomers 15A, 15B, and 15C are calculated to be 3.21, 3.38, and 3.35 eV. We suggest isomers 15A, 15B, and 15C to be the most probable isomers in the experiments. The spectral features of $CuSi_{15}^-$ are relatively broad in the experiments, which can be ascribed to the existence of multiple isomers. From the simulated DOS spectra in Figure 5, it is possible that isomers 15A, 15B, and 15C all contribute to the experimental spectrum. The structures of isomers 15A and 15B are similar to the most stable structures of $CuSi_{15}$ calculated by Chuang *et al.*[73] and Hossain *et al.*,[68] respectively.

M. $CuSi_{16}^-$

The first two isomers of $CuSi_{16}^-$ (16A and 16B) are both endohedral structures. Isomer 16B is higher than isomer 16A by 0.20 eV in energy. The exohedral structure of $CuSi_{16}^-$, isomer 16C, is much less stable than isomer 16A. It is higher than isomer 16A by ~1.94 eV. Thus, it is unlikely for isomer 16C to be present in the experiments. The VDEs of isomers 16A and 16B are calculated to be 3.35 and 3.61 eV, very close to the experimental value (3.51 eV). Thus, isomers 16A and 16B are the most probable isomers in the experiments. From the simulated DOS spectra in Figure 5, it is possible that both isomers 16A and 16B contribute to the experimental spectrum. The theoretical calculations of Chuang *et al.*[73] also show that the first two isomers of $CuSi_{16}$ are endohedral. According to our knowledge, $CuSi_{16}$ is the largest $CuSi_n$ cluster investigated by theoretical calculations in the literature.

N. $CuSi_{17}^-$

As for the most stable isomers of $CuSi_{17}^-$, isomers 17A and 17B are both endohedral structures and are close in energy, with isomer 17B higher than isomer 17A by only

0.15 eV. The Si_{17} cage of isomer 17A is formed by three four-membered rings and seven five-membered rings. The VDEs of isomers 17A and 17B are calculated to be 3.17 and 3.48 eV, respectively, in reasonable agreement with experimental value (3.63 eV). Isomers 17C, 17D, and 17E are much less stable than isomers 17A and 17B. Among them, isomers 17C and 17D are endohedral structures, while isomer 17E is an exohedral structure. From the simulated DOS spectra in Figure 5, it is possible that both isomers 17A and 17B contribute to the experimental spectrum of $CuSi_{17}^-$.

O. $CuSi_{18}^-$

The first three isomers of $CuSi_{18}^-$ are all endohedral structures. Isomers 18B and 18C are less stable than isomer 18A by 0.30 and 0.49 eV, respectively. Isomer 18C has the Cu atom sandwiched by two Si_6 rings to form a distorted hexagonal prism, then add six more silicon atoms to the waist of the hexagonal prism. Isomer 18D is an exohedral structure. It is less stable than isomer 18A by 0.50 eV. The VDE of isomer 18A is about 3.64 eV, in good agreement with the experimental value (3.7 eV). The VDEs of isomers 18B and 18C can also be considered as close to the experimental value. The VDE of isomer 18D is much lower than the experimental value. Considering the relative energies and the comparison of theoretical VDEs with the experimental value, we suggest isomer 18A to be the most probable isomer detected in the experiments. The simulated DOS spectrum of isomer 18A is in reasonable agreement with the experimental spectrum of $CuSi_{18}^-$.

Overall, the comparison of theoretical calculations with photoelectron experiments shows that the $CuSi_n^-$ clusters with n = 4–11 have exohedral structures and those with n = 12–18 have endohedral structures. It has been suggested that Cu atom adsorbing to small silicon clusters prefer to occupy a low coordination site.[54] The most stable structures of $CuSi_{4\text{-}8}^-$ found in this work are in agreement with that. Although some earlier theoretical calculations predicted $CuSi_{10}$ as a highly symmetric endohedral structure, our theoretical calculations and photoelectron experiments support an exohedral structure which is in agreement with theoretical calculations conducted by Xiao *et al.*[62] and the photodissociation experiment of $CuSi_{10}^+$ by Duncan and co-workers.[50] We found a double-chair endohedral structure to be the most stable structure for $CuSi_{12}^-$. That is in agreement with most of the theoretical calculations in the literature. It is also consistent with the Ar atom physisorption experiments and far-infrared spectroscopy experiments reported by Lievens and co-workers.[52,54] These authors observed that the ion intensity of $CuSi_n^+$ increased abruptly beyond n = 11 by Ar atoms physisorption technique, and proposed that $CuSi_{12}^+$ is the minimal size for the formation of the endohedral cluster. The far-infrared spectroscopy experiments conducted by the same authors further confirmed that the $CuSi_n^+$ clusters with $n \leq 11$ have exohedral structures. We also confirmed the earlier theoretical calculations that $CuSi_{14}^-$ has a C_{3h} symmetry structure with the Si_{14} cage composed of three four-membered rings and six five-membered rings. As mentioned earlier, in the photoelectron spectra of $CuSi_{12}^-$ and $CuSi_{14}^-$, the low bind features are relatively clear, which means these low binding features are well separated from the high binding features. That implies the $CuSi_{12}$ and $CuSi_{14}$ neutrals have relatively large HOMO-LUMO gaps. The special geometric structures of $CuSi_{12}^-$ and $CuSi_{14}^-$ found by theoretical calculations are consistent with the large band gaps observed in their photoelectron spectra.

It has been suggested[53] that some metal-doped silicon clusters can be formed by simply adding a metal atom to a bare silicon cluster or by substitution of a silicon atom with a metal atom without inducing significant change in the original structure of silicon clusters, but, in some cases, the doping of metal atom can cause complete rearrangement of the structure of silicon clusters. The formation of $CuSi_{12}^-$ and $CuSi_{14}^-$ belongs to the later one where the structures of Si_{12} and Si_{14} are completely rearranged due to the doping of Cu atoms.

V. CONCLUSIONS

Anion photoelectron spectroscopy experiments were conducted to investigate a series of copper-doped silicon clusters, $CuSi_n^-$ (n = 4–18). The VDEs and ADEs of the $CuSi_n^-$ (n = 4–18) clusters were estimated based on their photoelectron spectra. Extensive DFT calculations were performed to locate the low-lying isomers of $CuSi_n^-$ (n = 4–18). The structures of these $CuSi_n^-$ clusters were tentative assigned by comparison of theoretical calculations with experimental measurements. The geometry of $CuSi_{12}^-$ is confirmed to be a double-chair endohedral structure. $CuSi_{14}^-$ is a C_{3h} symmetry endohedral structure, in which the Si_{14} cage is composed of three four-membered rings and six five-membered rings. The $CuSi_n^-$ clusters with $n < 12$ are dominated by exohedral structures where the Cu atom occupies an exterior site, while the clusters with $n \geq 12$ are dominated by endohedral structures where the Cu atom is encapsulated into the Si_n cage.

ACKNOWLEDGMENTS

This work was supported by the Knowledge Innovation Program (Grant No. KJCX2-EW-H01) of the Chinese Academy of Sciences and the Natural Science Foundation of China (Grant Nos. 20853001, 21103202, and 10874007). The theoretical calculations were conducted on the ScGrid and Deepcomp7000 of the Supercomputing Center, Computer Network Information Center of Chinese Academy of Sciences.

[1] H. Hiura, T. Miyazaki, and T. Kanayama, Phys. Rev. Lett. **86**, 1733 (2001).
[2] M. Ohara, K. Koyasu, A. Nakajima, and K. Kaya, Chem. Phys. Lett. **371**, 490 (2003).
[3] W. J. Zheng, J. M. Nilles, D. Radisic, and K. H. Bowen, J. Chem. Phys. **122**, 071101 (2005).
[4] K. Koyasu, M. Akutsu, M. Mitsui, and A. Nakajima, J. Am. Chem. Soc. **127**, 4998 (2005).
[5] S. Neukermans, X. Wang, N. Veldeman, E. Janssens, R. E. Silverans, and P. Lievens, Int. J. Mass Spectrom. **252**, 145 (2006).
[6] M. Akutsu, K. Koyasu, J. Atobe, K. Miyajima, M. Mitsui, and A. Nakajima, J. Phys. Chem. A **111**, 573 (2007).
[7] K. Koyasu, J. Atobe, S. Furuse, and A. Nakajima, J. Chem. Phys. **129**, 214301 (2008).

[8]S. Furuse, K. Koyasu, J. Atobe, and A. Nakajima, J. Chem. Phys. **129**, 064311 (2008).
[9]P. Gruene, A. Fielicke, G. Meijer, E. Janssens, V. T. Ngan, M. T. Nguyen, and P. Lievens, ChemPhysChem **9**, 703 (2008).
[10]A. Grubisic, H. Wang, Y. J. Ko, and K. H. Bowen, J. Chem. Phys. **129**, 054302 (2008).
[11]A. Grubisic, Y. J. Ko, H. P. Wang, and K. H. Bowen, J. Am. Chem. Soc. **131**, 10783 (2009).
[12]J. T. Lau, K. Hirsch, P. Klar, A. Langenberg, F. Lofink, R. Richter, J. Rittmann, M. Vogel, V. Zamudio-Bayer, T. Moller, and B. von Issendorff, Phys. Rev. A **79**, 053201 (2009).
[13]H. G. Xu, Z. G. Zhang, Y. Feng, J. Y. Yuan, Y. C. Zhao, and W. J. Zheng, Chem. Phys. Lett. **487**, 204 (2010).
[14]H.-G. Xu, Z.-G. Zhang, Y. Feng, and W.-J. Zheng, Chem. Phy. Lett. **498**, 22 (2010).
[15]H.-G. Xu, M.-M. Wu, Z.-G. Zhang, Q. Sun, and W.-J. Zheng, Chin. Phys. B **20**, 043102 (2011).
[16]A. P. Yang, Z. Y. Ren, P. Guo, and G. H. Wang, J. Mol. Struct.: THEOCHEM **856**, 88 (2008).
[17]V. Kumar and Y. Kawazoe, Phys. Rev. Lett. **87**, 045503 (2001).
[18]S. N. Khanna, B. K. Rao, and P. Jena, Phys. Rev. Lett. **89**, 016803 (2002).
[19]V. Kumar and Y. Kawazoe, Phys. Rev. B **65**, 073404 (2002).
[20]A. N. Andriotis, G. Mpourmpakis, G. E. Froudakis, and M. Menon, New J. Phys. **4**, 78 (2002).
[21]J. Lu and S. Nagase, Phys. Rev. Lett. **90**, 115506 (2003).
[22]A. K. Singh, T. M. Briere, V. Kumar, and Y. Kawazoe, Phys. Rev. Lett. **91**, 146802 (2003).
[23]G. Mpourmpakis, G. E. Froudakis, A. N. Andriotis, and M. Menon, Phys. Rev. B **68**, 125407 (2003).
[24]G. Mpourmpakis, G. E. Froudakis, A. N. Andriotis, and M. Menon, J. Chem. Phys. **119**, 7498 (2003).
[25]P. Guo, Z. Y. Ren, F. Wang, J. Bian, J. G. Han, and G. H. Wang, J. Chem. Phys. **121**, 12265 (2004).
[26]A. Negishi, N. Kariya, K. Sugawara, I. Arai, H. Hiura, and T. Kanayama, Chem. Phys. Lett. **388**, 463 (2004).
[27]J. Wang and J. G. Han, J. Chem. Phys. **123**, 064306 (2005).
[28]J. U. Reveles and S. N. Khanna, Phys. Rev. B **74**, 035435 (2006).
[29]E. N. Koukaras, C. S. Garoufalis, and A. D. Zdetsis, Phys. Rev. B **73**, 235417 (2006).
[30]H. K. Yuan, H. Chen, A. S. Ahmed, and J. F. Zhang, Phys. Rev. B **74**, 144434 (2006).
[31]J. G. Han, R. N. Zhao, and Y. H. Duan, J. Phys. Chem. A **111**, 2148 (2007).
[32]Y. Ito, W. Fujita, T. Okazaki, T. Sugai, K. Awaga, E. Nishibori, M. Takata, M. Sakata, and H. Shinohara, ChemPhysChem **8**, 1019 (2007).
[33]L. Z. Kong and J. R. Chelikowsky, Phys. Rev. B **77**, 073401 (2008).
[34]R. Robles, S. N. Khanna, and A. W. Castleman, Phys. Rev. B **77**, 235441 (2008).
[35]J. Wang and J. H. Liu, J. Phys. Chem. A **112**, 4562 (2008).
[36]G.-F. Zhao, J.-M. Sun, Y.-Z. Gu, and Y.-X. Wang, J. Chem. Phys. **131**, 114312 (2009).
[37]R. Robles and S. N. Khanna, J. Chem. Phys. **130**, 164313 (2009).
[38]R. Robles and S. N. Khanna, Phys. Rev. B **80**, 115414 (2009).
[39]R.-N. Zhao, J.-G. Han, J.-T. Bai, and L.-S. Sheng, Chem. Phys. **378**, 82 (2010).
[40]A. K. Singh, V. Kumar, T. M. Briere, and Y. Kawazoe, Nano Lett. **2**, 1243 (2002).
[41]M. Menon, A. N. Andriotis, and G. Froudakis, Nano Lett. **2**, 301 (2002).
[42]A. N. Andriotis, G. Mpourmpakis, G. E. Froudakis, and M. Menon, New J. Phys. **4**, 14 (2002).
[43]A. K. Singh, V. Kumar, and Y. Kawazoe, J. Mater. Chem. **14**, 555 (2004).
[44]N. A. Borshch, N. S. Pereslavtseva, and S. I. Kurganskii, Semiconductors **40**, 1423 (2006).
[45]J. Bai and X. C. Zeng, NANO **2**, 109 (2007).
[46]U. Wahl, A. Vantomme, G. Langouche, and J. G. Correia, Phys. Rev. Lett. **84**, 1495 (2000).
[47]A. A. Istratov, T. Buonassisi, M. D. Pickett, M. Heuer, and E. R. Weber, Mater. Sci. Eng. B **134**, 282 (2006).
[48]A. Boukai, P. Haney, A. Katzenmeyer, G. M. Gallatin, A. A. Talin, and P. Yang, Chem. Phys. Lett. **501**, 153 (2011).
[49]M. B. Steven, J. Chem. Phys. **90**, 6306 (1989).
[50]J. B. Jaeger, T. D. Jaeger, and M. A. Duncan, J. Phys. Chem. A **110**, 9310 (2006).
[51]S. Neukermans, X. Wang, N. Veldeman, E. Janssens, R. E. Silverans, and P. Lievens, Int. J. Mass Spectrom. **252**, 145 (2006).
[52]E. Janssens, P. Gruene, G. Meijer, L. Woste, P. Lievens, and A. Fielicke, Phys. Rev. Lett. **99**, 063401 (2007).
[53]P. Gruene, A. Fielicke, G. Meijer, E. Janssens, V. T. Ngan, M. T. Nguyen, and P. Lievens, ChemPhysChem **9**, 703 (2008).
[54]V. T. Ngan, P. Gruene, P. Claes, E. Janssens, A. Fielicke, M. T. Nguyen, and P. Lievens, J. Am. Chem. Soc. **132**, 15589 (2010).
[55]C. Xiao and F. Hagelberg, J. Mol. Struct.: THEOCHEM **529**, 241 (2000).
[56]C. Y. Xiao, A. Abraham, R. Quinn, F. Hagelberg, and W. A. Lester, J. Phys. Chem. A **106**, 11380 (2002).
[57]I. V. Ovcharenko, W. A. Lester, C. Xiao, and F. Hagelberg, J. Chem. Phys. **114**, 9028 (2001).
[58]X. Liu, G. F. Zhao, L. J. Guo, X. W. Wang, J. Zhang, Q. Jing, and Y. H. Luo, Chin. Phys. **16**, 3359 (2007).
[59]A. Dkhissi, Int. J. Quantum Chem. **108**, 996 (2008).
[60]F. Hagelberg, I. Yanov, and J. Leszczynski, J. Mol. Struct.: THEOCHEM **487**, 183 (1999).
[61]C. Xiao, F. Hagelberg, I. Ovcharenko, and W. A. Lester, J. Mol. Struct.: THEOCHEM **549**, 181 (2001).
[62]C. Y. Xiao, F. Hagelberg, and W. A. Lester, Phys. Rev. B **66**, 075425 (2002).
[63]F. Hagelberg, C. Xiao, and W. A. Lester, Phys. Rev. B **67**, 035426 (2003).
[64]O. Ona, V. E. Bazterra, M. C. Caputo, M. B. Ferraro, P. Fuentealba, and J. C. Facelli, J. Mol. Struct.: THEOCHEM **681**, 149 (2004).
[65]G. K. Gueorguiev, J. M. Pacheco, S. Stafstrom, and L. Hultman, Thin Solid Films **515**, 1192 (2006).
[66]A. D. Zdetsis, Phys. Rev. B **75**, 085409 (2007).
[67]A. D. Zdetsis, E. N. Koukaras, and C. S. Garoufalis, J. Math. Chem. **46**, 971 (2009).
[68]D. Hossain, C. U. Pittman, and S. R. Gwaltney, Chem. Phys. Lett. **451**, 93 (2008).
[69]L. J. Guo, G. F. Zhao, Y. Z. Gu, X. Liu, and Z. Zeng, Phys. Rev. B **77**, 195417 (2008).
[70]J. G. Han and F. Hagelberg, J. Comput. Theor. Nanosci. **6**, 257 (2009).
[71]Y. Z. Lan and Y. L. Feng, Phys. Rev. A **79**, 033201 (2009).
[72]J. G. He, K. C. Wu, R. J. Sa, Q. H. Li, and Y. Q. Wei, Chem. Phys. Lett. **490**, 132 (2010).
[73]F. C. Chuang, C. C. Hsu, Y. Y. Hsieh, and M. A. Albao, Chin. J. Phys. **48**, 82 (2010).
[74]C. T. Lee, W. T. Yang, and R. G. Parr, Phys. Rev. B **37**, 785 (1988).
[75]A. D. Becke, J. Chem. Phys. **98**, 1372 (1993).
[76]M. J. Frisch, G. W. Trucks, H. B. Schlegel *et al.*, GAUSSIAN 03, Revision B.04, Gaussian, Inc., Pittsburgh, PA, 2003.
[77]Y. Wang and J. P. Perdew, Phys. Rev. B **44**, 13298 (1991).
[78]See supplementary material at http://dx.doi.org/10.1063/1.3692685 for a schematic drawing of the experimental setup, a typical anion mass spectrum of Cu/Si clusters, and the cartesian coordinates of the stable isomers of $CuSi_n^-$.
[79]J. T. David and C. H. Nicholas, J. Chem. Phys. **109**, 10180 (1998).
[80]J. Akola, M. Manninen, H. Hakkinen, U. Landman, X. Li, and L.-S. Wang, Phys. Rev. B **60**, R11297 (1999).
[81]R. B. King, Z. Phys. D **18**, 189 (1991).